LRRK2 phosphorylates moesin at Threonine-558: characterization of how Parkinson's disease mutants affect kinase activity

Mahaboobi Jaleel, R Jeremy Nichols, Maria Deak, David G Campbell, Frank Gillardon, Axel Knebel, Dario R Alessi

▶ To cite this version:

HAL Id: hal-00478755

https://hal.science/hal-00478755

Submitted on 30 Apr 2010

LRRK2 phosphorylates moesin at Thr558; characterisation of how Parkinson's disease mutants affect kinase activity.

By

Mahaboobi Jaleel[1], R. Jeremy Nichols[1], Maria Deak[1], David G. Campbell[1], Frank Gillardon[2], Axel Knebel[3] and Dario R. Alessi[1]

1. MRC Protein Phosphorylation Unit, MSI/WTB complex, University of Dundee, Dow Street, Dundee DD1 5EH, Scotland.
2. Boehringer Ingelheim Pharma GmbH & Co. KG, Birkendorfer Strasse 65, D-88397 Biberach an der Riss, Germany.
3. Kinasource Limited, Unit 9 South Dudhope Mill, 77 Douglas Street, Dundee DD1 5AN, Scotland.
Correspondence to DRA (d.r.alessi@dundee.ac.uk)
Tel +44 1382 344241
Fax +44 1382 223778

Short Title: moesin phosphorylation by LRRK2

Key Words: Protein kinase, KESTREL screening, Mass Spectrometry ERM proteins.

Abbreviations: GST, glutathione S-transferase; KESTREL, KinasE Substrate TRacking and Elucidation; LRRK2, Leucine Repeat Rich Kinase 2; LDS, Lithium dodecyl sulfate; MBP, Myelin basic protein; CRMP2, Collapsin response mediator protein 2; COR, C-terminal Of Ras of complex; PD, Parkinson's disease; GbpC, cGMP binding protein C; RIPK, Rho-Interacting Protein kinase; and ROCK-II, Rho associated kinase-2.

Author's contributions: Mahaboobi Jaleel undertook most of the experimentation presented in this study, planned experiments, contributed to writing the paper, and generated the figures; Jeremy Nichols, undertook experimentation showing that LRRK2 phosphorylated ezrin and radixin; Maria Deak generated the expression constructs and provided helpful discussion; David Campbell undertook the phosphopeptide mapping and provided helpful discussion; Frank Gillardon supported the KESTREL Screen and provided helpful discussion; Axel Knebel performed the KESTREL screen, participated in Discussion and helped to write the manuscript and Dario Alessi conceived of project, helped plan and interpret experiments and wrote the manuscript.

Abstract. Mutations in the Leucine Rich Repeat Kinase-2 (LRRK2) gene cause late-onset Parkinson's disease (PD). LRRK2, contains Leucine Rich Repeats, a GTPase domain, a COR domain, a kinase and a WD40 motif. Little is known about how LRRK2 is regulated, what its physiological substrates are or how mutations affect LRRK2 function. Thus far LRRK2 activity has only been assessed by autophosphorylation and phosphorylation of myelin basic protein, which is catalysed rather slowly. We undertook a KESTREL screen in rat brain extracts to identify proteins that were phosphorylated by an activated PD mutant of LRRK2 (G2019S). This led to the discovery that moesin, a protein which anchors the actin-cytoskeleton to the plasma membrane, is efficiently phosphorylated by LRRK2, at Thr558, a previously identified in vivo phosphorylation site that regulates the ability of moesin to bind actin. LRRK2 also phosphorylated ezrin and radixin that are related to moesin, at the residue equivalent to Thr558, as well as a peptide encompassing Thr558 (LRRKtide). We exploited these findings to determine how nine previously reported PD mutations of LRRK2 affected kinase activity. Only one of the mutations analysed, namely G2019S, stimulated kinase activity. Four mutations inhibited LRRK2 kinase activity (R1941H, I2012T, I2020T and G2385R), whereas the remainder (R1441C, R1441G, Y1699C and T2356I), did not influence activity. Therefore, the manner in which LRRK2 mutations induce PD, is more complex than previously imagined, and not only caused by an increase of LRRK2 kinase activity. Finally, we show that the minimum catalytically active fragment of LRRK2, requires an intact GTPase, COR and kinase domain as well as WD40 motif and C-terminal tail. This study suggests that moesin, ezrin and radixin may comprise LRRK2 substrates, findings that have been exploited to develop the first robust quantitative assay to measure LRRK2 kinase activity.

Introduction.

There has been much interest raised by the recent discovery that different autosomal dominant point mutations within the gene encoding for the Leucine Rich Repeat protein Kinase-2 (LRRK2), predispose humans to develop late-onset Parkinson's disease (PD, OMIM accession number 609007), with a clinical appearance indistinguishable from idiopathic PD [1-4]. The genetic analysis undertaken to date indicates that mutations in LRRK2 are relatively frequent, not only accounting for 5-10% of familial PD, but are also found in a significant proportion of sporadic PD cases [5, 6]. Little is known about how LRRK2 is regulated in cells, what are its physiological substrates and how mutations in LRRK2 cause or increase risk of PD. In mammals there are two isoforms of the LRRK protein kinase, LRRK1 (2038 residues) and LRRK2 (2527 residues). They belong to a protein family that has also been termed Roco [7]. Thus far, mutations in LRRK2, but not LRRK1 have been linked to PD.

The LRRK/Roco class of protein kinases was initially characterised in the slime mould *Dictyostelium discoideum*, as a protein termed GbpC (cGMP binding protein C), that comprised an unusual member of the Ras/GTPase superfamily, distinct from other small GTPase domains as it possesses other domains including a protein kinase [7, 8]. Subsequent studies suggested that GbpC regulates chemotaxis and cell polarity in *Dictyostelium* [9], but the physiological substrates for this enzyme have not been elucidated. The defining feature of the LRRK/Roco-proteins is that they possess Leucine Rich Repeat (LRR) motif, a Ras-like small GTPase, a region of high amino acid conservation that has been termed the C-terminal Of Ras of complex (COR) domain, and a protein kinase catalytic domain [7, 10]. The protein kinase domain of LRRK2 belongs to the tyrosine-like serine/threonine protein kinases and is most similar to the Rho-Interacting Protein kinases (RIPK), that play key roles in innate immunity signalling pathways [11]. Other domains are also found on specific members of the LRRK kinases. For example, the GbpC possesses an additional DEP (for Disheveled, EGL-10, Pleckstrin), cyclicGMP-binding and Ras-GEF domains that are not found in mammalian LRRK1 and LRRK2. Human LRRK1 possesses 3 ankyrin repeats at its N-terminus, whereas LRRK2 lacks these domains, but possesses a WD40 repeat located towards its C-terminus not found in LRRK1 [7].

Human LRRK2 consists of leucine rich repeats (residues 1010-1287), a small GTPase domain (residues 1335-1504), a COR domain (residues 1517-1843), a serine/threonine protein kinase domain (residues 1875-2132) and a motif that has low resemblance to a WD40 repeat (2231-2276) (Fig 1A). To date ~20 single amino acid substitution mutations have been linked to autosomal-dominant PD, and these have

3

been found within or in close proximity to conserved residues of the small GTPase, COR, protein kinase and WD40 domains [3, 4].

The most prevalent mutant form of LRRK2 accounting for ~6% of familial PD and 3% of sporadic PD cases in Europe, comprises an amino acid substitution of Gly2019 located within the conserved DYG-Mg^{2+}-binding motif, in subdomain-VII of the kinase domain, to a Ser residue [3]. Recent reports suggest that this mutation moderately enhances, ~2-3-fold, the autophosphorylation of LRRK2, as well as its ability to phosphorylate myelin basic protein [12, 13]. These findings suggest that over-activation of LRRK2 predisposes humans to develop PD, implying that drugs which inhibited LRRK2, could be utilised to delay the onset or even treat some forms of PD. The study of LRRK2 has been hampered by the difficulty in expressing active recombinant enzyme and by the lack of a robust quantitative assay. In this study we have developed a method to express active recombinant LRRK2 and utilised this in a KinasE Substrate TRacking and ELucidation (KESTREL) screen, that has recently been developed to identify physiological substrates of protein kinases (reviewed in [14]). This led to the identification of moesin, that when denatured was efficiently phosphorylated by LRRK2 at Thr558, a previously characterised physiologically relevant phosphorylation site. Although further investigation is required to determine whether moesin comprises a physiological substrate, we have utilised these findings to develop a robust and quantitative assay for LRRK2. Using this methodology we demonstrate that several LRRK2 mutations identified in patients with PD, either do not affect or actually inhibit, rather than activate LRRK2. We also demonstrate a requirement for an intact GTPase, COR and C-terminal region to maintain LRRK2 in a catalytically active conformation.

Materials and Methods.

Materials. Protease-inhibitor cocktail tablets were obtained from Roche; P81 phosphocellulose paper was from Whatman; [$β^{32}P$]-ATP and all protein chromatography media were purchased from Amersham Biosciences. Myelin basic protein (MBP) was from Invitrogen, Precast SDS polyacrylamide Bis-Tris gels were from Invitrogen; tissue culture reagents were from Life Technologies; Millipore Immobilon-P was from Fisher Scientific. Active rat ROCKII [residues 2-543] was expressed in baculovirus by the Division of Signal Transduction Therapy Unit (University of Dundee). The LRRKtide peptide (RLGRDKYKTLRQIRQ) was synthesised by Dr Graham Bloomberg at the University of Bristol.

Antibodies. The anti-GST was raised in sheep against the glutathione S-transferase protein. The secondary antibodies coupled to horseradish peroxidase used for immunoblotting were obtained from Pierce.

4

General methods. Tissue culture, transfection, immunoblotting, restriction enzyme digests, DNA ligations, and other recombinant DNA procedures were performed using standard protocols. All mutagenesis was carried out using the Quick-Change site-directed mutagenesis method (Stratagene). DNA constructs used for transfection were purified from *E.coli* DH5α using Qiagen plasmid Mega or Maxi kit according to the manufacturer's protocol. All DNA constructs were verified by DNA sequencing, which was performed by The Sequencing Service, School of Life Sciences, University of Dundee, Scotland, UK, using DYEnamic ET terminator chemistry (Amersham Biosciences) on Applied Biosystems automated DNA sequencers.

Buffers. Lysis Buffer contained 50 mM Tris/HCl pH 7.5, 1 mM EGTA, 1 mM EDTA, 1 % (w/v) Triton-X100, 1 mM sodium orthovanadate, 10 mM sodium- - glycerophosphate, 50 mM sodium fluoride, 5 mM sodium pyrophosphate, 0.27 M sucrose, 0.1 % (v/v) 2-mercaptoethanol and complete proteinase inhibitor cocktail (one tablet/50 ml, Boehringer). Buffer A contained 50 mM Tris/HCl pH 7.5, 0.1 mM EGTA and 0.1% (v/v) 2-mercaptoethanol. Extraction Buffer contained 50 mM Tris/HCl pH 7.5, 5% (v/v) glycerol, 10 mM 2-mercaptoethanol, 1 mM EDTA, 1 mM EGTA, 0.03% (v/v) Brij-35, complete proteinase inhibitor cocktail (one tablet/50 ml). Sample Buffer was 1X NuPAGE® LDS sample buffer (Invitrogen) containing 1% (by vol) 2-mercaptoethanol.

Plasmids. A full-length cDNA clone encoding LRRK2 corresponding to NCBI Acc. AAV63975 was a generous gift from Dr Michel Goedert (LMB Cambridge). The full length and the fragments of LRRK2 gene that were utilized in this study were amplified from the LRRK2 cDNA fragment, according to standard PCR methods, using KOD polymerase (Novagen). The resulting PCR products were subcloned into mammalian pEBG2T and pCMV5 expression vectors as *Bamh1-Not1* fragments. A cDNA encoding full-length as well as C-terminal fragments of human moesin (NCBI Acc. NP_002435) were amplified by PCR from an EST ordered from Geneservice (IMAGE clone 4908580). The PCR product was ligated into different expression vectors as *Not1-Not1* fragments.

Expression and purification of GST-LRRK2. Typically 10 to100 ten cm diameter dishes of HEK 293 cells, were cultured and each dish transfected with 5 μg of the pEBG-2T construct encoding wild type or different mutant forms of LRRK2 using the polyethylenimine method [15]. The cells were cultured for a further 36 h and lysed in 0.5 ml of ice-cold lysis buffer, the lysates pooled and centrifuged at 4°C for 10 min at 26,000 x g. The GST-fusion proteins were purified by affinity chromatography on glutathione-Sepharose (10 γl per dish of 293 cells) and were eluted in Buffer A containing 20 mM glutathione and 0.27 M sucrose. The enzyme was snap frozen in small aliquots and stored at -80 °C.

5

LRRK2 KESTREL screen. Brains derived from 50 rats were minced and homogenized with four volumes of Extraction Buffer. Insoluble material was sedimented by centrifugation for 20 min at 28, 000 x g at 4ºC, and the protein in the supernatant precipitated for 2 h by stirring with 60% (w/v) ammonium sulphate. The precipitated protein was collected by centrifugation for 20 min at 28,000 x g, resuspended in Extraction Buffer, desalted by chromatography on Sephadex-G25 fine into 30 mM MOPS pH 6.9, 10% (v/v) glycerol, 10 mM 2-mercaptoethanol, 0.03% (v/v) Brij-35 and chromatographed in the latter buffer on heparin-Sepharose. The flow-through of the heparin column was titrated with 1 M NaOH to pH 7.5 and applied onto a 8 ml Source 15 Q column, which was developed in 30 mM Tris/HCl pH 7.5, 10% (v/v) glycerol, 10 mM 2-mercaptoethanol, 0.03% (v/v) Brij-35 with a 136 ml gradient to 1 M NaCl. Aliquots of all fractions were diluted 10-fold in 50 mM Tris/HCl pH 7.5, 10 mM 2-mercaptoethanol, 10 μg/ml leupeptin, 1 mM Pefabloc, incubated at 65 ºC for 15 min prior to incubation for 5 min with 3 mM $MnCl_2$, 1 MBq/ml [^{32}P]-ATP in the absence or presence of 2 μg GST-LRRK2[1326-2527, G2019S] (purity of LRRK2 enzyme estimated at 2-5% of total protein). The reactions were terminated by addition of SDS-Sample Buffer, subjected to polyacrylamide gel electrophoresis and electro-transferred to Immobilon P. The membranes were dried and autoradiographed. All fractions and test aliquots were frozen at -80ºC. Substrate containing Q-fractions 5 and 6 were diluted five times in 30 mM Tris/HCl pH 8.2, 10% (v/v) glycerol, 10 mM 2-mercaptoethanol, 0.03% (v/v) Brij-35 and applied to a 1 ml Source 15 Q column. This column was developed in 30 mM Tris/HCl pH 7.5, 10% (v/v) glycerol, 10 mM 2-mercaptoethanol, 0.03% (v/v) Brij-35 with a 10 ml gradient to 1 M NaCl and 0.5 ml fractions were collected and aliquots were screened with LRRK2 as before. Substrate containing Q-fractions 6 and 7 were applied to a 120 ml Superdex-200 column and 1.2 ml aliquots were collected and screened. Substrate containing Superdex-fractions 12-15 were pooled, concentrated and desalted by filtration in a 2 ml VivaScience system. 4 μg aliquots were denatured or left native and tested for the presence of the substrate by phosphorylation in the presence or absence of LRRK2. The samples were electrophoresed on a polyacrylamide gel, stained with colloidal blue and analysed by autoradiography. The protein band corresponding to the substrate signal was excised, digested with trypsin and subjected to protein identification by Mass-Spectrometry Fingerprinting.

Expression and purification of human moesin in *E. coli*. The pGEX expression constructs encoding wild type and mutant forms of human moesin were transformed into *E.coli* BL21 cells and 1-litre cultures were grown at 37°C in Luria Broth containing 100 μg/ml ampicillin until the absorbance at 600 nm was 0.8. Induction of protein expression was carried out by adding 100 μM isopropyl-β-D-galactoside and

6

the cells were cultured for a further 16 hr at 26°C. Cells were isolated by centrifugation, resuspended in 15 ml of ice-cold Lysis Buffer and lysed in one round of freeze/thawing, followed by sonication to fragment DNA. The lysates were centrifuged at 4°C for 30 min at 26,000 x g, and the recombinant proteins were affinity purified on 0.2 ml of glutathione-Sepharose and were eluted in 0.4 ml of Buffer A containing 20 mM glutathione and 0.27 M sucrose.

Mapping the sites on Moesin phosphorylated by the G2019S LRRK2. Moesin (4 g) was treated at 65 °C for 15 min and then incubated at 30 ºC with 1.5 g of GST-LRRK2[1326-2527, G2019S] in Buffer A containing 10 mM MgCl$_2$ and 100 M [β^{32}P]-ATP (10000 cpm/pmol) in a total reaction volume of 50 l. The reaction was terminated after 40 min by adding Sample Buffer to a final concentration of 1% (w/v) LDS-10 mM dithiothreitol (DTT) and the samples heated at 100 °C for 1 min and cooled on ice. 4-vinylpyridine was added to a concentration of 50 mM, and the sample was left on a shaking platform for 30 min at room temperature to alkylate cysteine residues. The samples were subjected to electrophoresis on a BisTris 4-12% polyacrylamide gel, which was stained with colloidal blue and then autoradiographed. The phosphorylated moesin band was excised, cut into smaller pieces, washed sequentially for 15 min on a vibrating platform with 1 ml of the following: water, a 1:1 mixture of water and acetonitrile, 0.1 M ammonium bicarbonate, a 1:1 mixture of 0.2 M ammonium bicarbonate and acetonitrile and finally acetonitrile. The gel pieces were dried by speedi-vac and incubated in 0.1 ml of 50 mM ammonium bicarbonate, 0.1% (w/v) n-octyl-glucoside containing 1 g of mass spectroscopy grade trypsin (Promega). After 16 h, 0.1 ml of acetonitrile was added and the mixture incubated on a shaking platform for 10 min. The supernatant was removed and the gel pieces were further washed for 10 min in 0.3 ml of 50 mM ammonium bicarbonate, and 0.1% v/v trifluoroacetic acid. The combined supernatants, containing >90% of the ^{32}P-radioactivity, were chromatographed on a Vydac 218TP5215 C$_{18}$ column (Separations Group, Hesperia, CA) equilibrated in 0.1% v/v trifluoroacetic acid in water. The column was developed with a linear acetonitrile gradient (diagonal line) at a flow rate of 0.2 ml/min and fractions of 0.1 ml were collected. Phosphopeptides were further purified by Immobilised Metal-chelate Affinity Chromatography (IMAC) on Phospho-Select resin (Sigma).

Phosphopeptide sequence analysis. Isolated phosphopeptides were analysed by MALDI-TOF on and Applied Biosystems 4700 Proteomics Analyser using 5 mg/ml alpha-cyanno-4-hydroxy cinnamic acid as the matrix. Spectra were acquired in reflector mode and the phosphopeptides were analysed further by performing MALDI-TOF-TOF on selected masses. The characteristic loss of phosphoric acid (M-98 Da) from the parent phosphopeptide was seen. The site of phosphorylation of all

the ^{32}P-labelled peptides was determined by solid-phase Edman degradation on an Applied Biosystems 494C sequencer of the peptide coupled to Sequelon-AA membrane (Milligen) as described previously [16].

Assay of LRRK2 using moesin or MBP as substrates. Assays were set up in a total volume of 25 γ l of Buffer A containing 0.5-0.7 γ g of either wild type or mutant forms of LRRK2, 1 γ M moesin (full length or indicated mutants, that had been left on ice or incubated at 65 ^{o}C for 15 min prior to assay) or 1 γ M myelin basic protein, 10 mM MgCl$_2$ and 0.1 mM [β^{32}P]-ATP (300 cpm/pmol). After incubation for 30 min at 30 °C, the reactions were stopped by the addition of LDS-Sample Buffer. The incorporation of phosphate into moesin or MBP substrates as well as LRRK2 autophosphorylation was determined after electrophoresis of samples on a 4-12 %-polyacrylamide gels and autoradiography of the dried Coomassie Blue-stained gels. The phosphorylated substrates were also excised from the gel and ^{32}P-incorporation quantified by Cherenkov counting.

Assay of LRRK2 using LRRKtide as substrate. Assays were set up in a total volume of 50 γ l of Buffer A containing 0.5-0.7 γ g of either wild type or mutant forms LRRK2, 10 mM MgCl$_2$ and 0.1 mM [β^{32}P]-ATP (300 cpm/pmol) in the presence of 300 γ M or the indicated concentration of LRRKtide (RLGRDKYKTLRQIRQ) peptide substrate. After incubation for 30 min at 30 °C, reactions were terminated by applying 40 μl of the reaction mixture onto P81 phosphocellulose paper and phosphorylation of LRRKtide was quantified following washing the P81 phosphocellulose in 50 mM phosphoric acid and Cherenkov counting. One Unit (U) of LRRK2 activity was defined as the amount of enzyme that catalysed the incorporation of 1 nmol of ^{32}P into LRRKtide. Km and Vmax parameters were determined by performing the assay described above using varying concentration of LRRKtide. The Km and Vmax parameters were calculated using the Graph-Pad prism programme.

Immunoblotting. Samples were heated at 70° C for 5 min in Sample Buffer, subjected to polyacrylamide gel electrophoresis and transferred to a nitrocellulose membrane. Membranes were blocked for 30 min in 50 mM Tris/HCl pH 7.5, 0.15 M NaCl, 0.2% (v/v) Tween (TBST Buffer) containing 10% (w/v) skimmed milk. The membranes were probed with 1 μg/ml of anti-GST antibody for 16 h at 4°C in TBST Buffer containing 5% (w/v) skimmed milk. Detection was performed using horseradish peroxidase conjugated secondary antibodies and the enhanced chemiluminescence reagent.

8

Results.

Expression of an active fragment of LRRK2 for use in KESTREL. As a source of protein kinase for the KESTREL screen, we expressed GST-fusions of LRRK2 in 293 cells. Following affinity purification on glutathione-Sepharose, the expression level of full-length LRRK2 was low, but an LRRK2 fragment encompassing residues 1326-2527, lacking the Leu Rich Repeats, but still containing the GTPase, COR, kinase, WD40 and C-terminal tail was significantly higher (Fig 1A). The LRRK2[1326-2527] fragment autophosphorylated when incubated with magnesium and [β^{32}P]-ATP and phosphorylated myelin basic protein (MBP), albeit weakly (Fig 1B). A kinase-inactive mutant of LRRK2[1326-2527, D2017A] in which the Mg^{2+}-binding Asp residue was mutated, failed to autophosphorylate or phosphorylate MBP in a parallel reaction (Fig 1B). We also found that the common PD mutant LRRK2[1326-2527, G2019S] mentioned in the Introduction, displayed ~3-fold higher level of autophosphorylation and MBP phosphorylation compared with non-mutated LRRK2[1326-2527] (Fig 1B), consistent with previous work indicating that this mutation stimulated LRRK2 activity [12, 13].

LRRK2 KESTREL screen. To search for proteins in brain that are phosphorylated by LRRK2, an extract derived from 50 rats brains was precipitated with 60% (w/v) ammonium sulphate, desalted, chromatographed on heparin-Sepharose (Fig 2A), followed by Source-Q at pH 7.5 (Fig 2B) and Source-Q at pH 8.2 (Fig 2C) and finally on Superdex 200 gel filtration (Fig 2D & 2E). Aliquots of each column fraction were diluted in a reaction buffer and incubated for 15 min at 65 °C in order to inactivate endogenous protein kinases that might phosphorylate proteins and hence reduce background levels of phosphorylation that can otherwise interfere with the KESTREL analysis [17]. Each fraction was then incubated in the presence or absence of GST-LRRK2[1326-2527] or GST-LRRK2[1326-2527, G2019S] and [β^{32}P]-ATP as described in the Materials and Methods. Utilising purified non-mutated GST-LRRK2[1326-2527], no significant phosphorylation of any rat brain protein was detected (data not shown). Deploying the more active GST-LRRK2[1326-2527, G2019S] mutant, three proteins were observed to be phosphorylated (Figure 2). These proteins were purified, subjected to electrophoresis on a polyacrylamide gel and the identity of the Coomassie blue-stained band phosphorylated by LRRK2 in each preparation was established by tryptic peptide mass-spectral fingerprinting procedures (Fig 3). This revealed that the proteins phosphorylated by LRRK2 were collapsin response mediator protein-2 (CRMP2), creatine kinase and moesin. CRMP2 and creatine kinase were observed to be 50-100-fold more abundant in brain extracts than moesin (AK data not shown). To examine the relative phosphorylation of these proteins by LRRK2, similar amounts of purified, CRMP2, creatine kinase and moesin

9

proteins were phosphorylated with GST-LRRK2[1326-2527, G2019S] and under these conditions, moesin was phosphorylated to a markedly greater extent than CRMP2 or creatine kinase (Fig 3). Because CRMP2 and creatine kinase are highly abundant proteins and were phosphorylated by LRRK2 much less efficiently than moesin, we focused on studying the phosphorylation of moesin by LRRK2.

Mapping phosphorylated residues in moesin phosphorylated by LRRK2. We found that recombinant human GST-moesin expressed in *E.coli* that had been incubated at 65 °C for 15 min as performed in the KESTREL screen was phosphorylated by LRRK2 in a time dependent manner to a maximum stoichiometry of ~0.1 moles of phosphate per mole of moesin (Fig 4A). ^{32}P-moesin phosphorylated with LRRK2 was digested with trypsin and chromatographed on a C_{18} column to isolate ^{32}P-labelled phosphopeptides. This revealed two major peaks (P1 & P2) and one minor peak (P3) (Fig 4B). Solid phase Edman sequencing (Fig 4C) and mass spectrometry (Fig 4D & Supplementary Fig 1 for the MALDI-TOF-TOF spectrum of P2) of P1 and P2, established their identity as peptides phosphorylated at Thr558 and P3 as a peptide phosphorylated at Thr526. We next assessed how mutation of Thr526 and Thr558 in moesin affected phosphorylation by GST-LRRK2[1326-2527, G2019S]. Mutation of Thr526 moderately decreased phosphorylation of moesin by LRRK2, whereas mutation of Thr558 significantly reduced moesin phosphorylation (Fig 4E), indicating that this was the major site of phosphorylation. No phosphorylation of moesin was observed when both Thr526 and Thr558 residues were mutated.

Further analysis of the phosphorylation of moesin by LRRK2. Moesin is a member of the Ezrin/Radixin/Moesin (ERM) family of proteins that functions to anchor the actin cytoskeleton to the plasma membrane, and plays an important role in regulating membrane structure and organization [18, 19]. Moesin consists of a band Four-point-one/Ezrin/Radixin/Moesin (FERM) domain (residues 1 to 298) that interacts with several plasma membrane proteins [18, 19], as well as phosphoinositide 4,5 bisphosphate (PtdIns4,5P$_2$). The FERM domain on moesin is followed by an α-helical domain (residues 298 to 460), a flexible linker region (residues 460 to 489) and a conserved C-terminal tail (also termed C-ERMAD domain, residues 489 to 575). The last 30 amino acids of moesin encompassing Thr558, form an F-actin binding site [20-22]. Moesin and the other ERM proteins exist in at least two conformational states, namely an active "open" form capable of binding to membranes and F-actin and an inactive or dormant "closed" form, incapable of linking actin cytoskeleton to the plasma membrane, as the actin-binding site is masked. The structure of the closed state of moesin reveals that the FERM domain and C-terminal tail of moesin interact with each other, whilst in the open form the

10

FERM and C-terminal domains are dissociated [23]. Phosphorylation of moesin at Thr558, in conjunction to the FERM domain binding membrane proteins and perhaps to PtdIns(4,5)P$_2$, promotes the dissociation of the C-terminal tail from the FERM domain enabling moesin to bind to F-actin [24, 25]. The kinases that phosphorylate moesin at Thr558 have not been firmly established, although some candidates include the Rho associated kinase (ROCK) that phosphorylates the C-terminal tail of ERM proteins in vitro and when overexpressed in cells [26-28].

Previous reports found that the bacterially expressed C-terminal tail of moesin was phosphorylated by ROCK to a much greater extent than the full length moesin protein [26, 28]. This is presumably because when moesin is expressed in *E.coli* it will be in the closed conformation in which Thr558 is inaccessible for phosphorylation. We speculated that in the KESTREL screen, incubating moesin at 65 °C prior to phosphorylation, may have induced a conformational change that exposed Thr558. To investigate this, we studied how heating moesin expressed in *E.coli* affected its phosphorylation by LRRK2 (Fig 5A) as well as ROCK-II (Fig 5B) in parallel reactions. Strikingly, we found that neither LRRK2 nor ROCK-II were capable of phosphorylating moesin that had not been pre-incubated at a temperature of at least 60 °C (Fig 5A and 5B). In contrast, fragments of moesin lacking the FERM domain, could be phosphorylated by LRRK2 (Fig 5C) or ROCK-II (Fig 5D) in the absence of heat treatment prior to phosphorylation. Under the conditions employed, the moesin[400-577] C-terminal fragment was phosphorylated to ~2-fold greater extent than full length GST-moesin (Fig 5B).

Ezrin and Radixin are phosphorylated by LRRK2 at the residue equivalent to Thr558 of moesin. The amino acid sequence surrounding the Thr558 site of phosphorylation in moesin, is identical in ezrin and radixin, suggesting that these proteins will also be phosphorylated by LRRK2. To investigate this, we studied whether LRRK2 would phosphorylate full-length ezrin and radixin that had been expressed in *E.coli*. Similarly to full-length moesin, Ezrin and Radixin were only phosphorylated by LRRK2[1326-2527, G2019S] after they were heated at 70 °C (Fig 5D). Mutation of the residue equivalent to Thr558 in ezrin (Thr567) and Radixin (Thr564) to Ala, strongly reduced phosphorylation of these proteins by LRRK2 indicating that these are major phosphorylation sites. Under the conditions used GST-ezrin was phosphorylated at ~2-fold greater extent by LRRK2[1326-2527, G2019S] than GST-moesin and GST-radixin, suggesting that this might represent the best in vitro substrate to assess LRRK2 enzymic activity

Development of a peptide-based substrate assay for LRRK2. We next investigated whether LRRK2 could phosphorylate a short peptide substrate that encompassed the Thr567/Thr564/Thr558/ of ezrin/radixin/moesin (RLGRDKYK**T**LRQIRQ sequence

11

identical in all 3 proteins), in which the underlined Thr residue is equivalent to Thr558. We found that GST-LRRK2[1326-2527, G2019S] phosphorylated this peptide at ~3-fold higher initial rate than non-mutated GST-LRRK2[1326-2527], under conditions in which a kinase-inactive GST-LRRK2[1326-2527, D2017A] failed to phosphorylate the peptide (Fig 6A). The peptide was termed LRRKtide and was phosphorylated by both non-mutated GST-LRRK2[1326-2527] and GST-LRRK2[1326-2527, G2019S] with a similar Km of ~200 γ M (Fig 6B). The Vmax of phosphorylation of LRRKtide by GST-LRRK2[1326-2527, G2019S] was ~2.5-fold higher than that by non-mutated GST-LRRK2[1326-2527] (Fig 6B). The GST-LRRK2[1326-2527, G2019S] had a Vmax of 10 U/min/mg and the purity of the enzyme in this preparation was estimated at ~5% (Fig 6C), suggesting that a pure preparation of the LRRK2[G2019S] enzyme would phosphorylate LRRKtide with specific activity of 200 U/min/mg, a respectable rate for a relatively active kinase phosphorylating a favourable substrate.

Side by side assay of PD mutant forms of LRRK2. Utilising the assays elaborated on in this study, we next compared the activity of nine mutant forms of LRRK2 that have been reported in humans suffering from PD (reviewed in [3]). The mutations studied were found in the GTPase domain (R1441C, R1441G), COR region (Y1699C), kinase domain (R1914H, I2012T, G2019S, I2020T) and in a region of the C-terminal tail that lies beyond the WD40 repeat (T2356I, G2385R) (Fig 7A). We found that only the commonly observed G2019S mutation significantly stimulated LRRK2 autophosphorylation as well as phosphorylation of moesin, LRRKtide and MBP (Fig 7B). Four mutants (R1441C, R1441G, Y1699C and T2356I), possessed similar activity as non-mutated LRRK2 in all assays (Fig 7B). Two out of the four mutations in the kinase domain (R1914H, I2012T) were nearly inactive, displaying only marginally greater activity than the kinase-inactive LRRK2[D2017A] used as a control. A third kinase domain mutant (I2020T), possessed significantly less activity than non-mutated LRRK2, but higher activity that the R1914H and I2012T mutants. Intriguingly, one of the two C-terminal tail LRRK2 mutations (G2385R), also possessed very low catalytic activity in all assays (Fig 7B).

Defining the minimum fragment of LRRK2 that retains protein kinase activity. We compared the activity of full length and mutant forms of LRRK2 lacking specific domains. Wild type full length LRRK2 possessed similar activity towards the moesin, LRRKtide and MBP substrates, as the did the LRRK2[1326-2527] fragment utilised in the rest of this study. A mutant lacking either the GTPase domain (LRRK2[1541-2527]) or both the GTPase and COR domains (LRRK2[1856-2527]) displayed no autophosphorylation and did not phosphorylate any substrate. Moreover, LRRK2 mutants lacking either the C-terminal WD40 domain (LRRK2[1326-2149]) or just the

12

seven C-terminal amino acids ([LRRK2[1326-2520]), were also inactive. Consistent with the notion that the GTPase, COR, WD40 and C-terminal region of LRRK2 are required for its activity, a fragment of LRRK2 encompassing only the kinase domain (LRRK2[1856-2145]) was devoid of any kinase activity (Fig 8).

Discussion.

In this study we have employed the most active mutant G2019S form of LRRK2 encompassing residues 1326-2527 for a kinase substrate screen in brain and identified moesin and the related ezrin and radixin proteins as substrates for this enzyme. A peptide encompassing the phosphorylation site Thr558, whose sequence is identical in moesin, ezrin and radixin was efficiently phosphorylated by LRRK2. Based on these findings we developed the first robust quantitative assay for LRRK2 and analysed the requirements for catalytic kinase activity of LRRK2, by comparing a set of point mutants and deletions and to establish how mutations of LRRK2 found in PD patients impacted on enzyme activity. This study is another example for the usefulness of the KESTREL approach for finding substrates for poorly characterised protein kinases. Further work is required to evaluate whether moesin, ezrin or radixin comprise physiological substrates for LRRK2. To do this rigorously, it would be vital to assess phosphorylation of moesin at Thr558 in LRRK2 knock-out/down mice or cells or in knock-in mice expressing the G2019S mutation. It may also be necessary to knock-out/down the expression of the LRRK1, that most likely would also phosphorylate ERM proteins efficiently.

Were the ERM proteins found to comprise physiological substrates for LRRK2, the role that these might play in neurodegeneration and development of PD would require further investigation. In this regard, moesin and radixin have been implicated in playing a key role in regulating neurite outgrowth, as neurones that are deficient in these proteins display a marked reduction of growth cone size, disappearance of radial striations, retraction of the growth cone, and a marked disorganization of actin filaments that invade the central region of growth cones [29]. Recent studies also demonstrate that overexpression of the activated G2019S LRRK2 mutant induces a progressive reduction in neurite length and branching both in primary neuronal cell culture and in the rat nigrostriatal pathway, whereas LRRK2 deficiency leads to increased neurite length and branching [30]. Taken together these data suggest that deregulation of moesin phosphorylation by mutant LRRK2 might contribute to the early loss of dopaminergic axon terminals in PD. In humans inactivating mutations in a gene encoding a protein related to moesin, termed merlin, cause neurofibromatosis type 2, a form of cancer affecting predominantly the nervous system [31]. Little is known regarding the identity of the kinases that phosphorylate

13

the residue equivalent to Thr558 in the merlins's C-terminal tail. It would be of interest to investigate whether LRRK2 could phosphorylate merlin at this residue.

Our results confirm that the most common G2019S LRRK2 PD mutation enhances kinase activity, a conclusion that is consistent with two recent studies in which LRRK2 activity was assessed by autophosphorylation and phosphorylation of MBP [12, 13]. Our kinetic analysis with LRRKtide, also indicates that the G2019S mutation stimulates LRRK2 activity by increasing the catalytic Vmax constant rather than enhancing substrate-binding Km affinity. It would be interesting to crystallise the LRRK2 catalytic domain and determine how substitution of the conserved Gly residue nearby the Mg^{2+} Asp residue in sub-domain VII of the kinase domain could stimulate the catalytic efficiency of phosphorylation. Analysis of the 518 human kinases indicates that two protein kinases (TSSK1, BUBR1), as well as seven predicted inactive pseudokinases (KSR2, STLK6, RSKL1, SgK071, Domain2_GCN2, SgK269, SgK196), have a Gly to Ser substitution motifs at subdomain VII of their catalytic domain [11, 32]. It would be interesting to establish how mutation of the TSSK1 and BUBR1 subdomain-VII Ser residue to Gly, affected activity of these kinases. It is possible that such amino acid substitutions were used as an evolutionary mechanism to increase the basal activity of these enzymes. It might also be interesting to investigate the effect of Gly to Ser mutation in other protein kinases.

Our data indicate that not all PD mutations stimulate the activity of LRRK2. We found that four PD mutations R1441C, R1441G (located in GTPase domain), Y1699C (located in COR domain) and T2356I (located in C-terminal tail) did not significantly influence LRRK2 kinase activity. Moreover, three mutations R1941H, I2012T (located in kinase domain) and G2385R (located in the C-terminal tail) markedly inhibited LRRK2 kinase activity. Another PD mutation I2020T (in the residue located next to the Gly2019) reduced LRRK2 autophosphorylation and phosphorylation of MBP and moesin, but to a lower extent than the R1941H, I2012T and G2385R mutations (Fig 7). A recent report indicated that the Y1699C mutation possessed ~50% increased autophosphorylation compared to the wild type protein [33]. Although our data may indicate that this mutant possesses marginally greater activity than the wild type protein (Fig 7), it is significantly less active than the G2019S mutant. Another report judged the ability of the I2020T LRRK2 mutant to autophosphorylate to a ~40% higher level than wild type LRRK2 [34], which contrasts to our findings that this mutant possess lower activity. The reasons for this discrepancy are not clear, but measurement of autophosphorylation is potentially unreliable, not least as it is difficult to ensure that these assays are linear. Moreover, autophosphorylation of a protein kinase is not always proportional to the intrinsic

14

activity of the enzyme. Our results indicate that not all mutations exert their effects in the same manner as the G2019S mutation, which increases protein kinase activity. It is possible that some of the mutations exert their effects by interfering with the cellular interaction of LRRK2 with regulatory binding partners and/or alter LRRK2 cellular stability or localisation. The finding that some mutations reduce kinase activity, indicate that inhibition of LRRK2 might also have the potential to lead to degeneration of dopaminergic neurones and development of PD. If this was the case, it would suggest that the therapeutic efficacy of LRRK2 inhibitors might be limited to treatment of patients with activating G2019S LRRK2 mutations and that doses of such drugs would need to be utilised that do not reduce the activity of the disease causing LRRK2[G2019S] enzyme below basal levels.

Our work also demonstrates that an intact C-terminal tail of LRRK2 is required for activity, as truncation of only the seven C-terminal residues of this region ablated LRRK2 activity (Fig 8). We also found that the G2385R PD mutation located C-terminal to the WD40 motif inactivated LRRK2 kinase activity (Fig 7). Recent work suggest that this mutation, that is especially prevalent in ethnic Chinese Taiwanese populations, may represent a polymorphism that increases the risk of developing PD rather than a PD causative mutation [35]. The C-terminal region of LRRK2, apart from the WD40 motif, possesses no homology to any other known protein or other functional domain and further analysis is required to investigate the mechanism by which this domain can regulate LRRK2.

In summary the results in this study define the minimum fragment of LRRK2 that retains protein kinase activity and also demonstrate that in vitro, LRRK2 efficiently phosphorylates moesin at Thr558. Although further work is required to establish whether moesin comprises a physiological substrate of LRRK2, our findings will aid the functional analysis of LRRK2 by providing a more quantitative and robust methodology to assess LRRK2 protein kinase activity. They will also enable a better characterisation of how different PD mutations affect LRRK2 activity and assist drug discovery programmes in screening for LRRK2 inhibitors for the treatment of PD.

McLauchlan and James Hastie for generation and purification of antibodies and ROCK-II. We thank the Association for International Cancer Research, Diabetes UK, the Medical Research Council, the Moffat Charitable Trust and the pharmaceutical companies supporting the Division of Signal Transduction Therapy Unit (AstraZeneca, Boehringer-Ingelheim, GlaxoSmithKline, Merck & Co. Inc, Merck KgaA and Pfizer) for financial support.

References.

1   Paisan-Ruiz, C., Jain, S., Evans, E. W., Gilks, W. P., Simon, J., van der Brug, M., Lopez de Munain, A., Aparicio, S., Gil, A. M., Khan, N., Johnson, J., Martinez, J. R., Nicholl, D., Carrera, I. M., Pena, A. S., de Silva, R., Lees, A., Marti-Masso, J. F., Perez-Tur, J., Wood, N. W. and Singleton, A. B. (2004) Cloning of the gene containing mutations that cause PARK8-linked Parkinson's disease. Neuron **44**, 595-600

2   Zimprich, A., Biskup, S., Leitner, P., Lichtner, P., Farrer, M., Lincoln, S., Kachergus, J., Hulihan, M., Uitti, R. J., Calne, D. B., Stoessl, A. J., Pfeiffer, R. F., Patenge, N., Carbajal, I. C., Vieregge, P., Asmus, F., Muller-Myhsok, B., Dickson, D. W., Meitinger, T., Strom, T. M., Wszolek, Z. K. and Gasser, T. (2004) Mutations in LRRK2 cause autosomal-dominant parkinsonism with pleomorphic pathology. Neuron **44**, 601-607

3   Mata, I. F., Wedemeyer, W. J., Farrer, M. J., Taylor, J. P. and Gallo, K. A. (2006) LRRK2 in Parkinson's disease: protein domains and functional insights. Trends Neurosci. **29**, 286-293

4   Taylor, J. P., Mata, I. F. and Farrer, M. J. (2006) LRRK2: a common pathway for parkinsonism, pathogenesis and prevention? Trends Mol. Med. **12**, 76-82

5   Farrer, M., Stone, J., Mata, I. F., Lincoln, S., Kachergus, J., Hulihan, M., Strain, K. J. and Maraganore, D. M. (2005) LRRK2 mutations in Parkinson disease. Neurology **65**, 738-740

6   Zabetian, C. P., Samii, A., Mosley, A. D., Roberts, J. W., Leis, B. C., Yearout, D., Raskind, W. H. and Griffith, A. (2005) A clinic-based study of the LRRK2 gene in Parkinson disease yields new mutations. Neurology **65**, 741-744

7   Marin, I. (2006) The Parkinson disease gene LRRK2: evolutionary and structural insights. Mol. Biol. Evol. **23**, 2423-2433

8   Goldberg, J. M., Bosgraaf, L., Van Haastert, P. J. and Smith, J. L. (2002) Identification of four candidate cGMP targets in Dictyostelium. Proc. Natl. Acad. Sci. U S A **99**, 6749-6754

9   Bosgraaf, L., Russcher, H., Smith, J. L., Wessels, D., Soll, D. R. and Van Haastert, P. J. (2002) A novel cGMP signalling pathway mediating myosin phosphorylation and chemotaxis in Dictyostelium. Embo. J. **21**, 4560-4570

10   Bosgraaf, L. and Van Haastert, P. J. (2003) Roc, a Ras/GTPase domain in complex proteins. Biochim. Biophys. Acta **1643**, 5-10

11   Manning, G., Whyte, D. B., Martinez, R., Hunter, T. and Sudarsanam, S. (2002) The protein kinase complement of the human genome. Science **298**, 1912-1934

12   West, A. B., Moore, D. J., Biskup, S., Bugayenko, A., Smith, W. W., Ross, C. A., Dawson, V. L. and Dawson, T. M. (2005) Parkinson's disease-associated

mutations in leucine-rich repeat kinase 2 augment kinase activity. Proc. Natl. Acad. Sci. U S A **102**, 16842-16847

13 Greggio, E., Jain, S., Kingsbury, A., Bandopadhyay, R., Lewis, P., Kaganovich, A., van der Brug, M. P., Beilina, A., Blackinton, J., Thomas, K. J., Ahmad, R., Miller, D. W., Kesavapany, S., Singleton, A., Lees, A., Harvey, R. J., Harvey, K. and Cookson, M. R. (2006) Kinase activity is required for the toxic effects of mutant LRRK2/dardarin. Neurobiol. Dis. **23**, 329-341

14 Cohen, P. and Knebel, A. (2006) KESTREL: a powerful method for identifying the physiological substrates of protein kinases. Biochem. J. **393**, 1-6

15 Durocher, Y., Perret, S. and Kamen, A. (2002) High-level and high-throughput recombinant protein production by transient transfection of suspension-growing human 293-EBNA1 cells. Nucleic Acids Res. **30**, E9

16 Campbell, D. G. and Morrice, N. A. (2002) Identification of Protein Phosphorylation Sites by a Combination of Mass Spectrometry and Solid Phase Edman Sequencing. J. Biomol. Techn. **13**, 121-132

17 Troiani, S., Uggeri, M., Moll, J., Isacchi, A., Kalisz, H. M., Rusconi, L. and Valsasina, B. (2005) Searching for biomarkers of Aurora-A kinase activity: identification of in vitro substrates through a modified KESTREL approach. J. Proteome Res. **4**, 1296-1303

18 Bretscher, A., Edwards, K. and Fehon, R. G. (2002) ERM proteins and merlin: integrators at the cell cortex. Nat. Rev. Mol. Cell Biol. **3**, 586-599

19 Polesello, C. and Payre, F. (2004) Small is beautiful: what flies tell us about ERM protein function in development. Trends Cell Biol. **14**, 294-302

20 Gary, R. and Bretscher, A. (1995) Ezrin self-association involves binding of an N-terminal domain to a normally masked C-terminal domain that includes the F-actin binding site. Mol. Biol. Cell **6**, 1061-1075

21 Pestonjamasp, K., Amieva, M. R., Strassel, C. P., Nauseef, W. M., Furthmayr, H. and Luna, E. J. (1995) Moesin, ezrin, and p205 are actin-binding proteins associated with neutrophil plasma membranes. Mol. Biol. Cell **6**, 247-259

22 Turunen, O., Wahlstrom, T. and Vaheri, A. (1994) Ezrin has a COOH-terminal actin-binding site that is conserved in the ezrin protein family. J. Cell Biol. **126**, 1445-1453

23 Pearson, M. A., Reczek, D., Bretscher, A. and Karplus, P. A. (2000) Structure of the ERM protein moesin reveals the FERM domain fold masked by an extended actin binding tail domain. Cell **101**, 259-270

24 Huang, L., Wong, T. Y., Lin, R. C. and Furthmayr, H. (1999) Replacement of threonine 558, a critical site of phosphorylation of moesin in vivo, with aspartate activates F-actin binding of moesin. Regulation by conformational change. J. Biol. Chem. **274**, 12803-12810

25 Nakamura, F., Huang, L., Pestonjamasp, K., Luna, E. J. and Furthmayr, H. (1999) Regulation of F-actin binding to platelet moesin in vitro by both phosphorylation of threonine 558 and polyphosphatidylinositides. Mol. Biol. Cell **10**, 2669-2685

26 Matsui, T., Maeda, M., Doi, Y., Yonemura, S., Amano, M., Kaibuchi, K., Tsukita, S. and Tsukita, S. (1998) Rho-kinase phosphorylates COOH-terminal threonines of ezrin/radixin/moesin (ERM) proteins and regulates their head-to-tail association. J. Cell Biol. **140**, 647-657

17

27   Oshiro, N., Fukata, Y. and Kaibuchi, K. (1998) Phosphorylation of moesin by rho-associated kinase (Rho-kinase) plays a crucial role in the formation of microvilli-like structures. J. Biol. Chem. **273**, 34663-34666

28   Tran Quang, C., Gautreau, A., Arpin, M. and Treisman, R. (2000) Ezrin function is required for ROCK-mediated fibroblast transformation by the Net and Dbl oncogenes. EMBO J. **19**, 4565-4576

29   Paglini, G., Kunda, P., Quiroga, S., Kosik, K. and Caceres, A. (1998) Suppression of radixin and moesin alters growth cone morphology, motility, and process formation in primary cultured neurons. J. Cell Biol. **143**, 443-455

30   MacLeod, D., Dowman, J., Hammond, R., Leete, T., Inoue, K. and Abeliovich, A. (2006) The familial Parkinsonism gene LRRK2 regulates neurite process morphology. Neuron **52**, 587-593

31   McClatchey, A. I. and Giovannini, M. (2005) Membrane organization and tumorigenesis--the NF2 tumor suppressor, Merlin. Genes Dev. **19**, 2265-2277

32   Boudeau, J., Miranda-Saavedra, D., Barton, G. J. and Alessi, D. R. (2006) Emerging roles of pseudokinases. Trends Cell Biol. **16**, 443-452

33   West, A. B., Moore, D. J., Choi, C., Andrabi, S. A., Li, X., Dikeman, D., Biskup, S., Zhang, Z., Lim, K. L., Dawson, V. L. and Dawson, T. M. (2007) Parkinson's disease-associated mutations in LRRK2 link enhanced GTP-binding and kinase activities to neuronal toxicity. Hum. Mol. Genet. **16**, 223-232

34   Gloeckner, C. J., Kinkl, N., Schumacher, A., Braun, R. J., O'Neill, E., Meitinger, T., Kolch, W., Prokisch, H. and Ueffing, M. (2006) The Parkinson disease causing LRRK2 mutation I2020T is associated with increased kinase activity. Hum. Mol. Genet. **15**, 223-232

35   Farrer, M. J., Stone, J. T., Lin, C. H., Dachsel, J. C., Hulihan, M. M., Haugarvoll, K., Ross, O. A. and Wu, R. M. (2007) Lrrk2 G2385R is an ancestral risk factor for Parkinson's disease in Asia. Parkinsonism Relat. Disord.

Figure Legends.

Figure. 1. Generation of an active LRRK2 fragment for KESTREL screen. (A) (Upper panel) Schematic representation of the domain structure of LRRK2 showing predicted functional domains. Numbering of residues corresponds to human LRRK2 (accession number AAV63975). Abbreviations LRR (leucine-rich repeat), COR (C-terminal Of Ras conserved motif), KD (Serine/threonine protein kinase domain). (Lower panel) 293 cells were transfected with constructs encoding the indicated forms of GST-LRRK2. 36 h post-transfection, LRRK2 kinases were affinity purified and analysed by electrophoresis on a polyacrylamide gel and stained with colloidal blue to quantify relative protein levels. GST-LRRK2 was assayed by measuring autophosphorylation of LRRK2 following electrophoresis on a polyacrylamide gel and subsequent autoradiography of the colloidal blue-stained bands corresponding MBP or LRRK2. Asterisks on lower panel correspond to LRRK2 coomassie-staining bands. (B), As in (A) except that LRRK2 was also assayed by measuring phosphorylation of MBP. Abbreviation: KI, kinase-inactive (D2017A) LRRK2. Similar results were obtained in three separate experiments.

Figure 2. The LRRK2[G2019S] KESTREL screen. (A to E) Proteins extracted from rat brain, that did not bind to Heparin-Sepharose, were sequentially chromatographed on the indicated columns. The specified fractions were phosphorylated in the presence (+) or absence (-) of GST-LRRK2[1326-2527, G2019S] and [β^{32}P]-ATP as described in the Materials and Methods. Phosphorylation of substrates was analysed following the polyacrylamide electrophoresis of the samples and autoradiography. The identity of the moesin, CRMP2 and creatine kinase as the phosphorylated substrates was established by mass spectrometry in Fig 3.

Figure 3. Identification of moesin as an LRRK2 substrate. Fractions 10-15 of a Superdex 200 column containing the 62 kDa substrate (CRMP2) that interacted with Heparin-Sepharose (Fig 2A) that was further purified in Source-Q prior to Superdex, fractions 12-15 of a Superdex 200 column containing a 68 kDa substrate (Moesin) (Fig 2) and fraction 11 of a Q-column containing a 43 kDa substrate (creatine kinase) were concentrated using VivaScience spin filter. The samples were phosphorylated in the absence (-) or presence (+) of GST-LRRK2[1326-2527, G2019S] and [β^{32}P]-ATP as described in the Materials and Methods. Phosphorylation of substrates was analysed following the polyacrylamide electrophoresis of the samples and autoradiography. All samples were run on the same gel, but the bands shown were cut and pasted together to simplify the data. The black lines indicate where the gel was cut. The colloidal blue stained bands that were phosphorylated by LRRK2 (marked

19

with *), were excised from the gel, digested in-gel with trypsin, and their identities determined by tryptic peptide mass-spectral fingerprint. Mascot score is where a value of >63 is considered significant (P<0.05).

Fig. 4. Identification of residues on moesin that are phosphorylated by LRRK2.
(A) *E. coli* expressed moesin was incubated at 65^0C for 15 min, prior to phosphorylation with GST-LRRK2[1326-2527, G2019S] and $[\beta^{32}P]$-ATP for the indicated times. Phosphorylation of the moesin protein was determined following electrophoresis on a polyacrylamide gel and subsequent autoradiography of the colloidal blue-stained bands corresponding to moesin. Similar results were obtained in three separate experiments. (B) ^{32}P-labelled moesin after phosphorylation with the GST-LRRK2 [1326-2527, G2019S] for 40 min, was digested with trypsin and chromatographed on a C_{18} column. Fractions containing the major ^{32}P-labelled tryptic peptide (P1), peptide (P2) and peptide (P3) are shown and no other major ^{32}P-labelled peptides were observed in other fractions of the chromatography. (C) The indicated peptides were subjected to solid-phase sequencing and the ^{32}P-radioactivity released after each cycle of Edman degradation was measured. (D) Peptides were also analysed by MALDI–TOF and MALDI-TOF–TOF mass spectrometry (the latter spectra for Peptide P2 is shown in Supplementary Fig 1) and the inferred amino acid sequence and the site of phosphorylation denoted by (p) is indicated, together with the observed and theoretical mass of each peptide. (E) As in (A) except the indicated wild type and mutant forms of moesin were phosphorylated with GST-LRRK2[1326-2527, G2019S] for 30 min. Similar results were obtained in two separate experiments.

Fig. 5. Analysis of phosphorylation of moesin by LRRK2 (A) *E. coli* expressed GST-moesin (1 γ M) was incubated at the indicated temperatures for 15 min, prior to phosphorylation with GST-LRRK2[1326-2527, G2019S] (upper panel) or ROCK-II (lower panel) at 30 °C. Phosphorylation of the moesin protein was determined following electrophoresis on a polyacrylamide gel and subsequent autoradiography of the colloidal blue-stained bands corresponding to moesin. (B & C) As in (A) except the indicated wild type and truncated forms of moesin (all at a concentration of 1 γ M) were "heat denatured" by incubating at 70 °C for 15 min prior to phosphorylation with either active GST-LRRK2[1326-2527, G2019S] or kinase-inactive (KI) GST-LRRK2[1326-2527, D2017A] or ROCKII. Similar results were obtained in two separate experiments. Numbers above the Gel bands indicate the relative phosphorylation compared to MBP (B) or moesin[500-577] (C) not heat denatured. (D) As above, except that phosphorylation of full length wild type and indicated

20

mutants of *E. coli* expressed GST-Ezrin and GST-Radixin by GST-LRRK2[1326-2527, G2019S] was analysed.

Fig. 6. Generation of a peptide substrate for LRRK2. (A) 293 cells were transfected with constructs encoding the indicated forms of active and kinase-inactive (KI, D2017A) GST-LRRK2. 36 h post-transfection, LRRK2 kinases were affinity purified and analysed by electrophoresis on a polyacrylamide gel and stained with colloidal blue to quantify relative protein levels. GST-LRRK2 (1 γ g of total protein from each preparation) was assayed by measuring phosphorylation of the LRRKtide peptide (RLGRDKYKTLRQIRQ) at 300 γ M, as described in the Materials and Methods. Results of the kinase catalytic assays are presented as the mean catalytic activity ± S.D. of assays carried out in triplicate. The results presented are representative of 2 to 3 independent experiments. (B) As in (A) except that concentrations of LRRKtide varied to enable calculation of the Vmax and Km enzymatic parameters. (C) 2 γ g of the indicated forms of GST-LRRK2 assayed in (A) was analysed by electrophoresis on a polyacrylamide gel that was stained with colloidal blue.

Fig. 7. Analysis of PD disease LRRK2 mutants. (A) Schematic representation showing the location of nine PD causing mutations on LRRK2 that we analysed (abbreviations as in Fig 1). (B) The non-mutated and indicated mutant forms of GST-LRRK2[1326-2527] were expressed in 293 cells and affinity purified on glutathione-Sepharose. 2.0 γ g of each preparation was analysed by electrophoresis on a polyacrylamide gel that was stained with colloidal blue to quantify relative protein levels. Each preparation was assayed by measuring autophosphorylation as well as phosphorylation of MBP, moesin [500-577] and LRRKtide peptide. The data for LRRKtide phosphorylation are presented as the mean specific activity (Units per mg of total protein within purified GST-LRRK2 preparation) ± S.D. of assays carried out in triplicate. The results presented are representative of 2 to 3 independent experiments. Abbreviations: WT, wild type; KI, kinase-inactive (D2017A) LRRK2

Fig. 8. Role of non-kinase domains in regulating LRRK2 activity. (Upper panel) Schematic representation of the domain structure of LRRK2 showing predicted functional domains and numbering of residues corresponds to human LRRK2 residue (accession number AAV63975). Abbreviations are as in Fig 1. (Lower panels) The wild type and indicated fragments of GST-LRRK2 were expressed in 293 cells and affinity purified on glutathione-Sepharose. 1.0 γ g of each preparation was analysed by electrophoresis on a polyacrylamide gel that analysed by electrophoresis on a

21

polyacrylamide gel and immunoblotted with an anti-GST antibody to quantify relative protein levels. Each preparation was also assayed by measuring autophosphorylation as well as phosphorylation of MBP, moesin [500-577] and LRRKtide. The data for the LRRKtide assay are presented as the mean specific activity (Units per mg of total protein within purified GST-LRRK2 preparation) ± S.D. for assays carried out in triplicate. The results presented are representative of 2 independent experiments. Abbreviations: WT, wild type; KI kinase-inactive (D2017A) LRRK2.
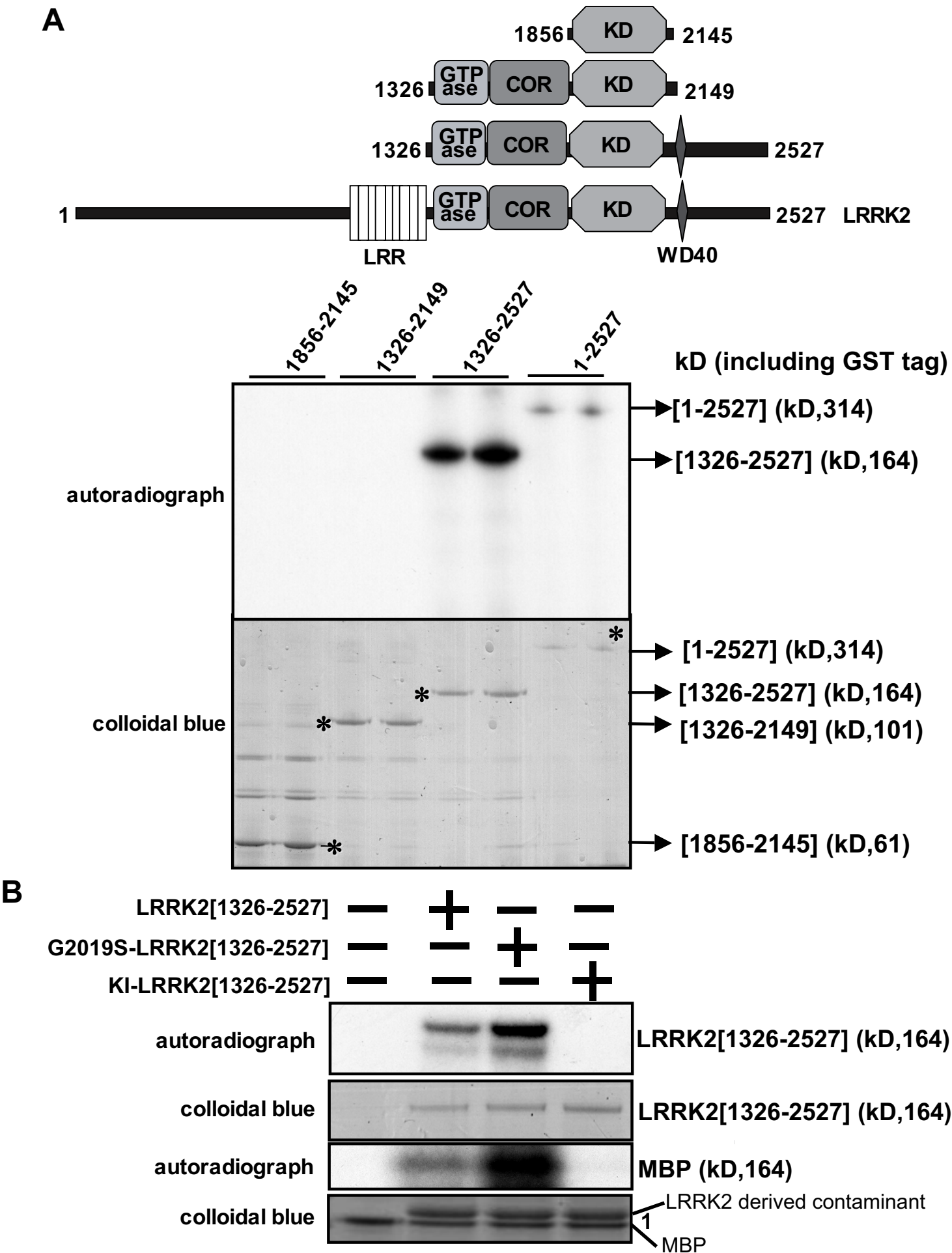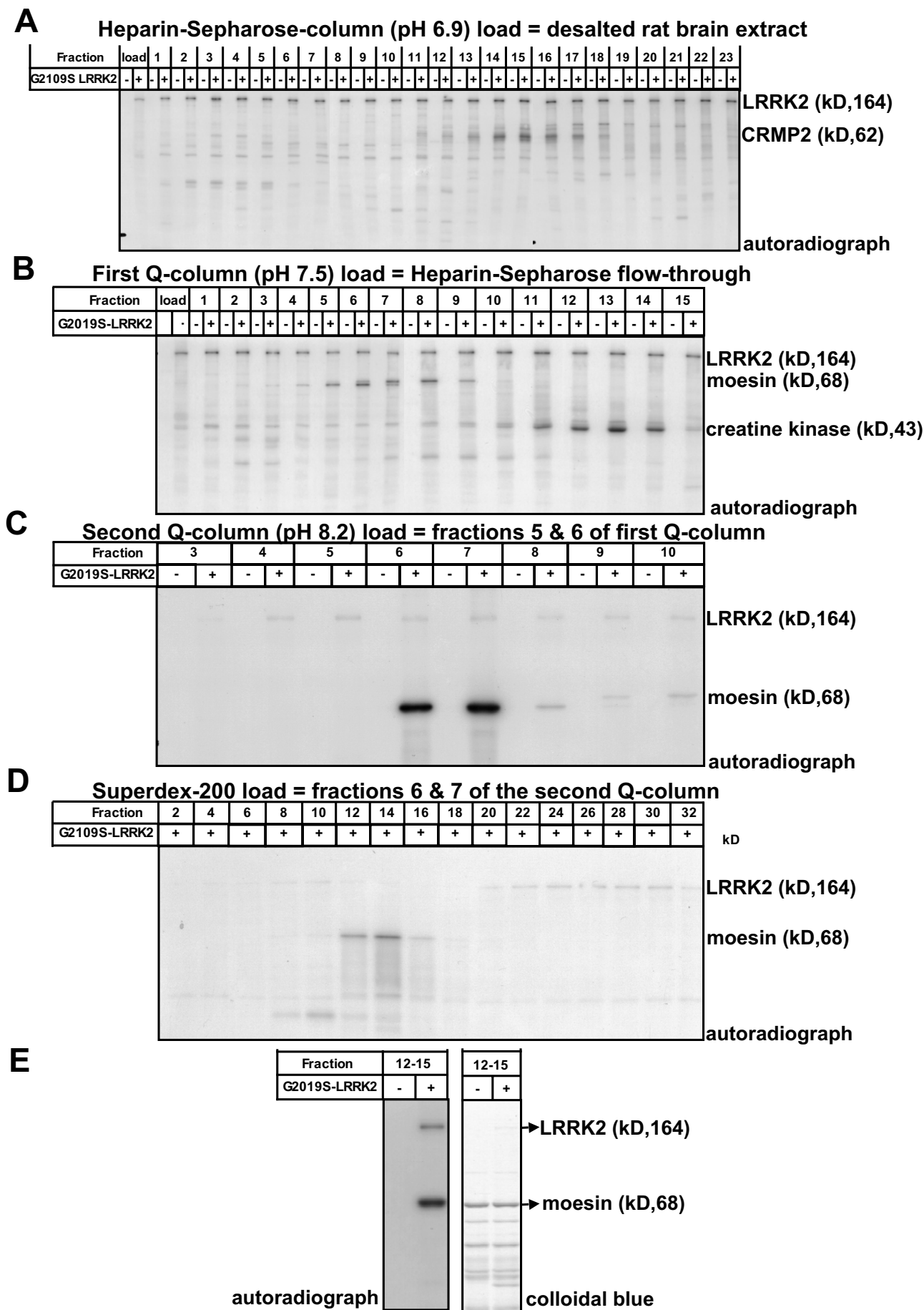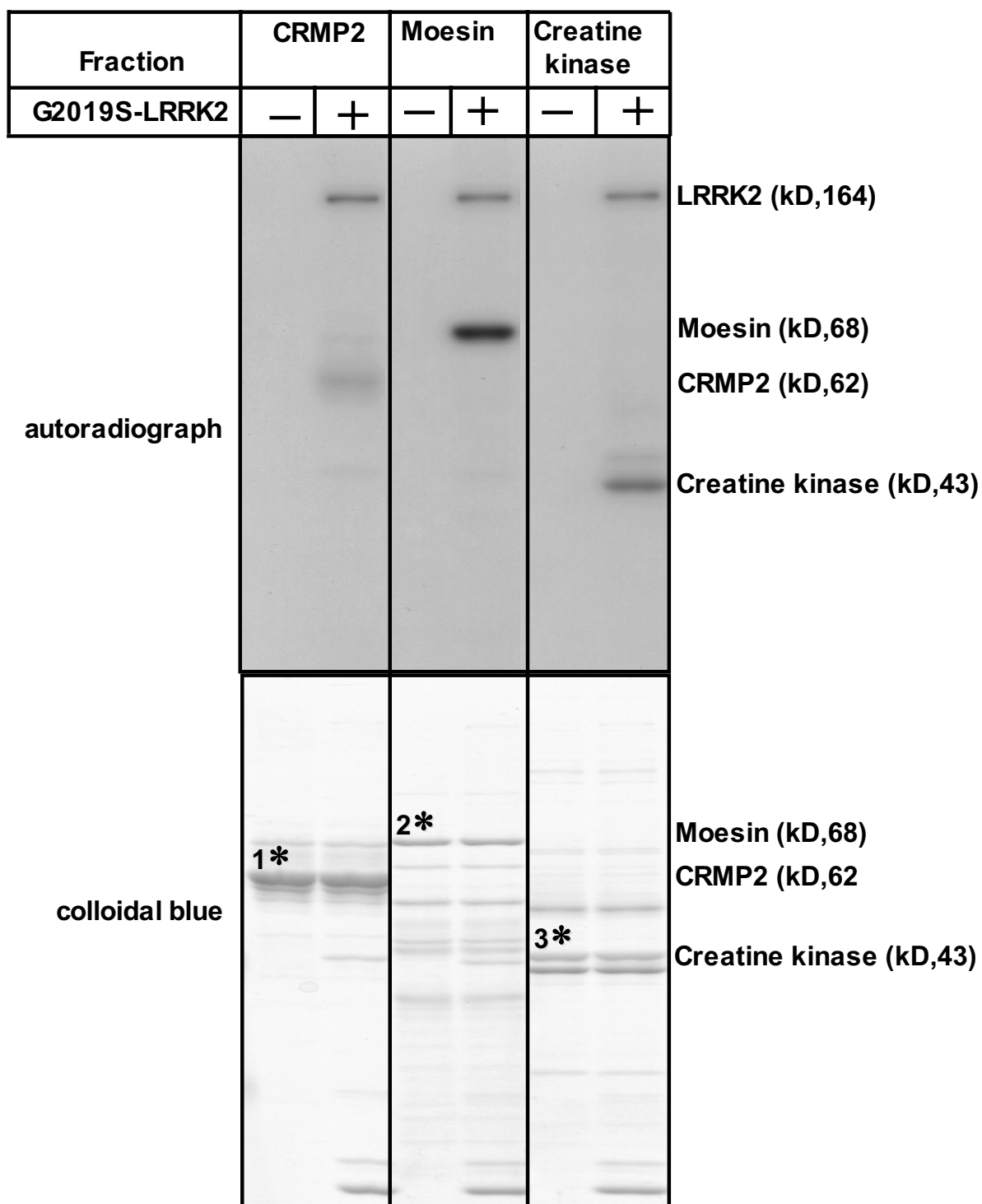
Figure 1

A

Heparin-Sepharose-column (pH 6.9) load = desalted rat brain extract

LRRK2 (kD,164)
CRMP2 (kD,62)
autoradiograph

B

First Q-column (pH 7.5) load = Heparin-Sepharose flow-through

LRRK2 (kD,164)
moesin (kD,68)
creatine kinase (kD,43)
autoradiograph

C

Second Q-column (pH 8.2) load = fractions 5 & 6 of first Q-column

LRRK2 (kD,164)
moesin (kD,68)
autoradiograph

D

Superdex-200 load = fractions 6 & 7 of the second Q-column

LRRK2 (kD,164)
moesin (kD,68)
autoradiograph

E

→ LRRK2 (kD,164)
→ moesin (kD,68)
autoradiograph   colloidal blue

Figure 2

Sample ID	Protein name	% Sequence coverage	Mascot score	Swiss prot number
1	CRMP2 (Collapsin response mediator Protein 2)	63	1733	P47942
2	Moesin	60	1550	P26038
3	Creatine kinase	50	829	P12277

Figure 3

A

B

C

D

Peptide	Phosphopeptide	Observed Mass[M+H]$^+$	Theoretical Mass[M+H]$^+$
Moesin P1	YKT(p)LR	760.4059	760.3759
Moesin P2	DKYKT(p)LR	1003.5416	1003.4978
Moesin P3	ALT(p)SELANAR	1125.6119	1125.5305

E

Figure 4

Figure 5

A

B

Kinase	WT LRRK2 [1326-2527]	G2019S LRRK2 [1326-2527]
V_{max} (U/min/mg)	5.5± 0.5	12 ± 0.5
Km (µM)	199 ± 43	201 ± 24

C
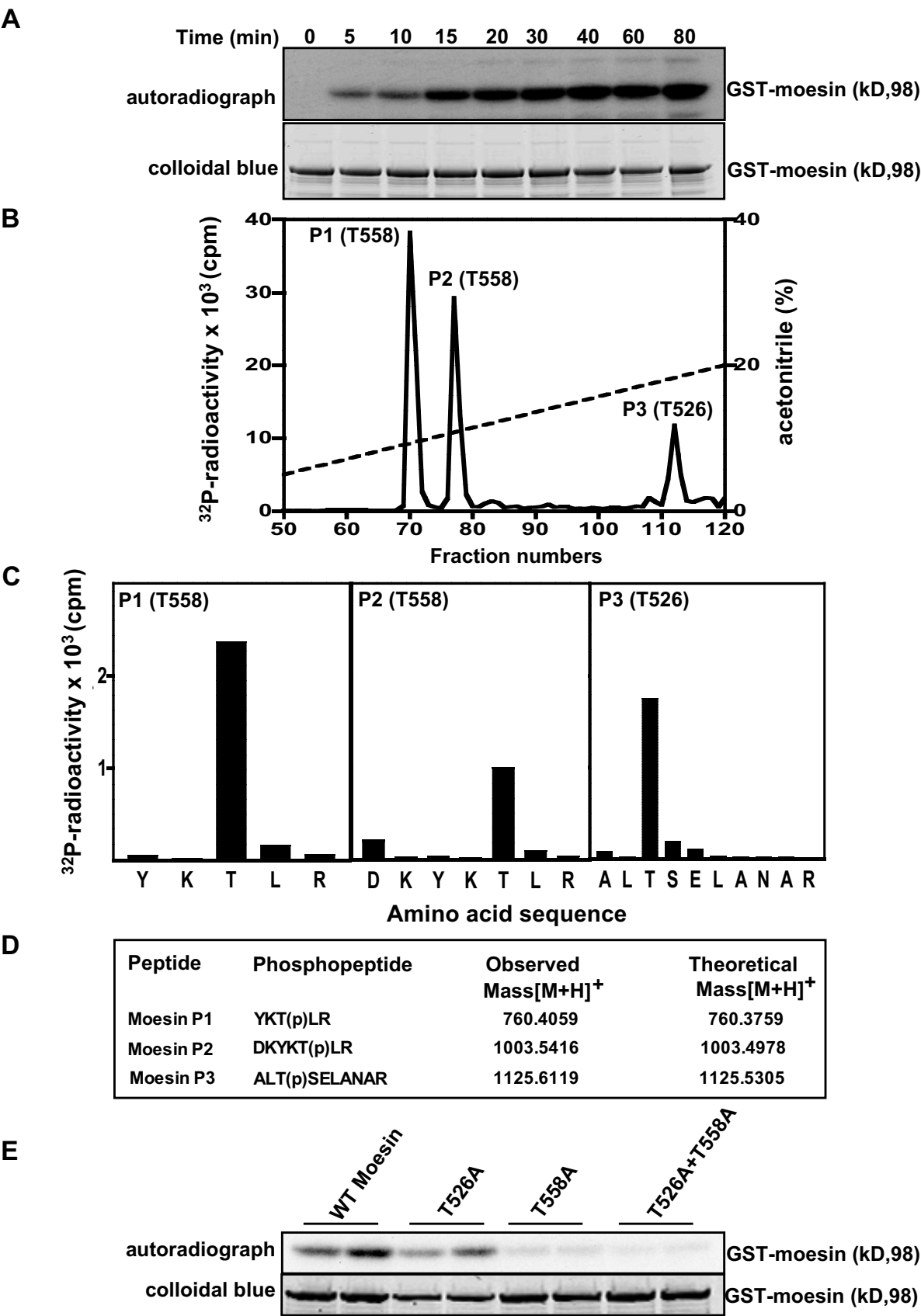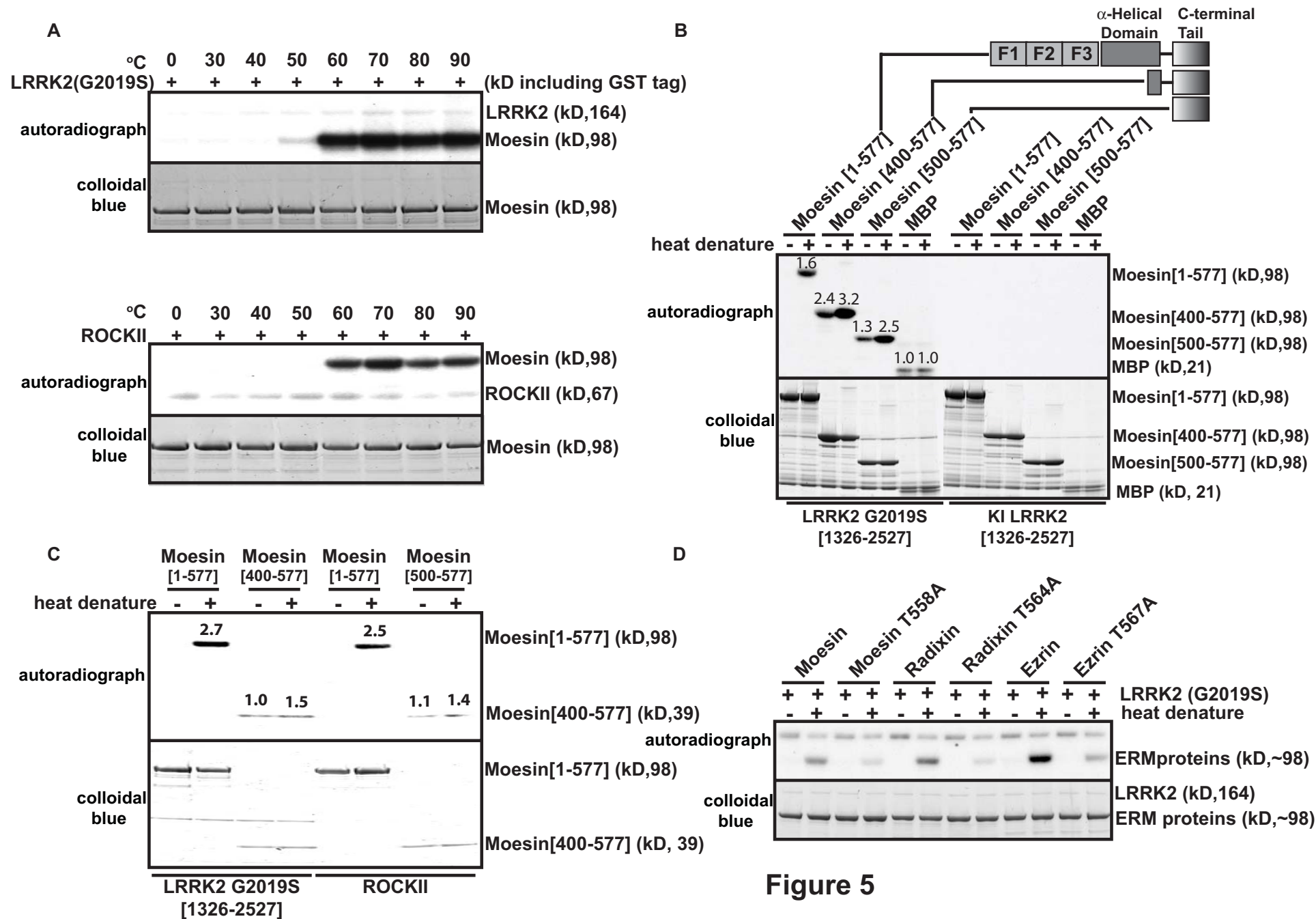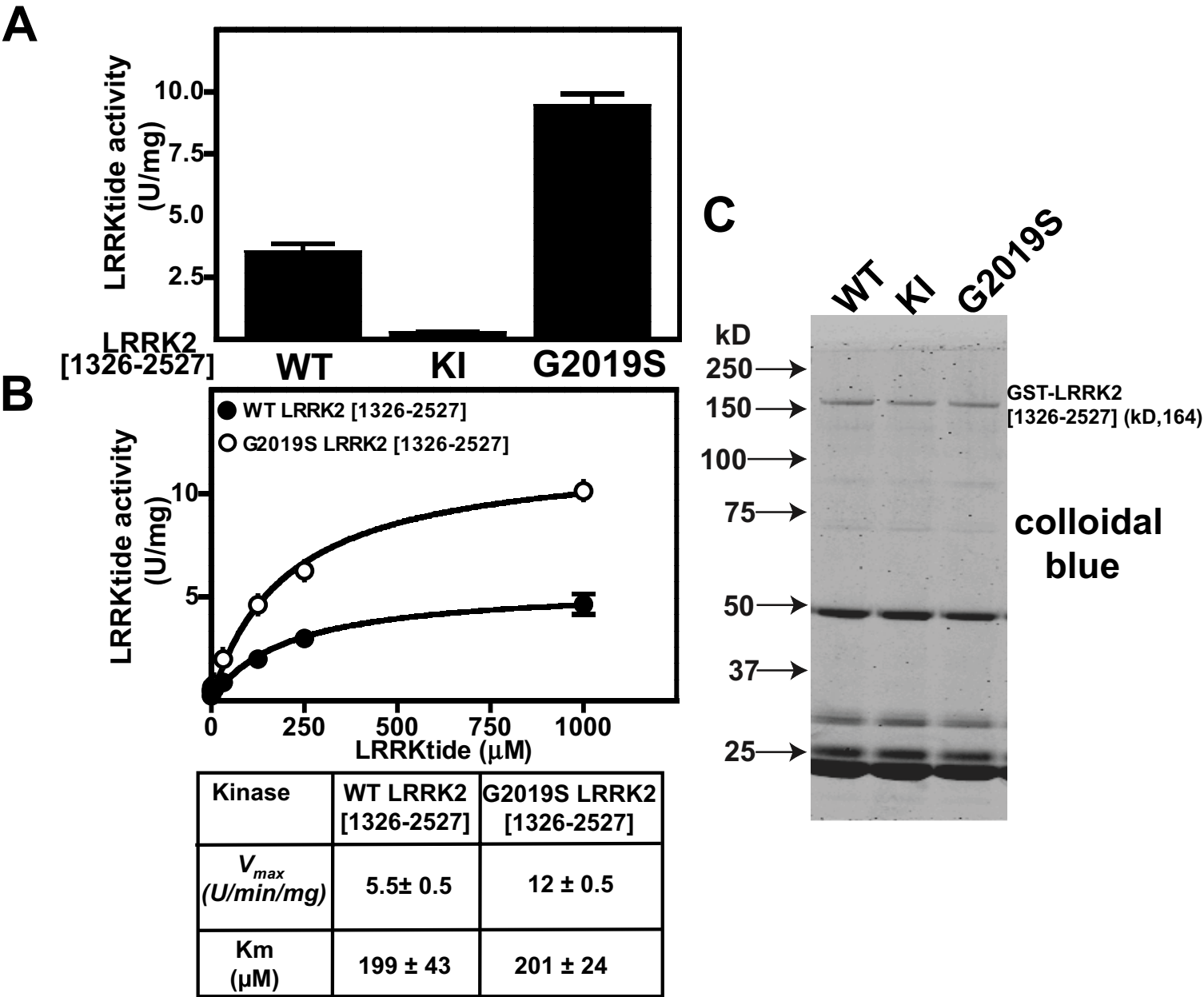
Figure 6

Figure 7

Figure 8